

---

EFDA-JET-CP(04)06-40

C. Sozzi, A. Bruschi, A. Simonetto, E. DeLaLuna, J. Fessey, V. Riccardo  
and JET-EFDA Contributors

# Optical Design of the Oblique ECE Antenna System for JET

---



# Optical Design of the Oblique ECE Antenna System for JET

C. Sozzi<sup>1</sup>, A. Bruschi<sup>1</sup>, A. Simonetto<sup>1</sup>, E. DeLaLuna<sup>2</sup>, J. Fessey<sup>3</sup>, V. Riccardo<sup>3</sup>  
and JET-EFDA Contributors\*

<sup>1</sup>*Istituto di Fisica del Plasma, Associazione EURATOM-ENEA-CNR, Milano, Italy*

<sup>2</sup>*Asociación EURATOM-CIEMAT, CIEMAT, Madrid, Spain*

<sup>3</sup>*EURATOM-UKAEA Association, Culham Science Centre, Abingdon, UK*

\* *See annex of J. Pamela et al, "Overview of Recent JET Results and Future Perspectives",  
Fusion Energy 2002 (Proc. 19th IAEA Fusion Energy Conference, Lyon (2002)).*

Preprint of Paper to be submitted for publication in Proceedings of the  
23rd SOFT Conference,  
(Venice, Italy 20-24 September 2004)

“This document is intended for publication in the open literature. It is made available on the understanding that it may not be further circulated and extracts or references may not be published prior to publication of the original when applicable, or without the consent of the Publications Officer, EFDA, Culham Science Centre, Abingdon, Oxon, OX14 3DB, UK.”

“Enquiries about Copyright and reproduction should be addressed to the Publications Officer, EFDA, Culham Science Centre, Abingdon, Oxon, OX14 3DB, UK.”

## **ABSTRACT**

Systematic disagreements between ECE and Thomson Scattering diagnostics observed in various fusion devices have substantiated the proposal of the so called Oblique ECE diagnostics on JET. This layout allows the study of the electron distribution function at low energies revealing deviations from the Maxwellian distribution. This paper is devoted to the design of the quasi optical antenna for the diagnostics. The physics requirements imply two lines of sight at about 10 and 20 degrees respectively from the magnetic field gradient. Severe geometrical constraints are imposed by the mounting method of the antenna. The design strategy and physical optics calculations used to validate it are presented.

## **1. MOTIVATION**

The correct measurement of the plasma temperature has been an important issue since the beginning of thermonuclear fusion research. The introduction of Electron Cyclotron Emission (ECE) diagnostics as routinely available electron temperature measurement in tokamak and stellarators provided a major burst in the understanding of the plasma behavior in fusion relevant conditions. The availability of effective and powerful additional heating systems opened very high temperature scenarios bringing to light new phenomena related to the electron temperature measurements, actually arising the question of what exactly the diagnostic itself is measuring. In particular some systematic disagreements between ECE and Thomson Scattering diagnostics have been observed in the presence of NBI and ICRF heating (TFTR and JET)[1,2], and ECR heating (FTU) [3,4], probably due to deviation of the electron population from Maxwellian-bulk distribution [5].

These observations have substantiated the proposal of the so called Oblique ECE diagnostics on JET, in which the ECE radiation is detected along lines of sight at small angle with respect to the magnetic field gradient, instead of the perpendicular view used in the standard ECE measurements. This layout allows the study of the electron distribution function at low energies revealing any non Maxwellian shape.

## **2. DESIGN STRATEGY**

The physics requirements imply two lines of sight at about 10 and 20 degrees respectively in the toroidal direction with respect to the perpendicular to the magnetic field. Severe geometrical constraints are imposed by the mounting method of the antenna, inserted in the vacuum vessel together with the group of six oversized waveguides devoted to Reflectometry and Oblique ECE itself and their surrounding structure. The two Oblique ECE waveguides share the same horizontal plane with one reflectometer waveguide, and are at the opposite sides of the structure with respect to it. The antenna has been designed with three flat mirrors and an ellipsoidal one, the last being shared by the two lines of sight. The mirror arrangement was optimized using electromagnetic calculations performed at several frequencies in the band of the diagnostic, extending from 100 to 400GHz.

The chosen solution was to use two symmetric external waveguides in a row, leaving free the central one (only cut 50-66mm with respect to the untouched row). This solution is the more compact in length and leaves room for the external supports.

## 2.1 CLEARANCES

A requirement for any design solution is to avoid interferences between the mirrors and the antenna pattern of the waveguide used for other microwave diagnostics, especially for the adopted configuration with the waveguide left in the centre. The optimal clearances for 100GHz (4\*beam radius at the given distance from the waveguide aperture) evaluated with simple gaussian optics are about 50, 65 and 70mm at distances of 50, 90 and 100mm respectively.

The most critical interference for the configuration in figure 1 occurs at about 90mm (mirror n.2). This configuration is possible only if a 3\*beam radius clearance is accepted (corresponding to 38.5, 51.9 and 55.8mm respectively) and if this mirror is slightly cut at the bottom together with the top of the lower mirrors in the figure (n. 0 and n. 3). The impact on the ECE oblique pattern at low frequencies has been evaluated with the physical optics calculations presented below.

## 2.2 MIRROR CURVATURE

The spatial resolution (in poloidal and toroidal directions) of the oblique ECE diagnostics is improved if a focusing effect is introduced in the antenna system; in order to start the optimisation process an indicative calculation based on gaussian optics was done assuming a distance of the curved mirror of 140mm from the waveguide aperture, and a reference frequency of 180GHz. The beam radius (defined as the radius where the power density drops to  $1/e^2$  of the maximum) at 1500mm from the mirror was then calculated as a function of the focal length of the last mirror. This process produces as the best result a beam radius of 60mm for a focal length of 500mm. Assuming a 500mm focal length mirror, in figure 2 the beam radius at 1500mm from the mirror is plotted as a function of wave frequency.

In order to optimise the focal length, two alternatives could be taken: to use two different ellipsoidal mirrors, one for each beam (mirror 2 for the 10° beam, mirror 1 for the 20° beam) or to use only the mirror 3 to focus both the beams, keeping flat all the other mirrors. This last solution resulted to be about 25% more effective in focusing the beams at the distance of the plasma edge from the antenna, accepting to have slightly astigmatic beams. The ellipsoid for the last mirror was obtained as a compromise between the optimal ellipsoids for the two beams. As a practical rule, the average incidence angle and the average path length of the central rays emerging from the two waveguide apertures were selected as defining the location of the first focus of the ellipsoidal surface, at 630.67mm from the mirror centre. The second focus is located at 1550.33mm from the first one, at 10.50° down the axis of the central waveguide. The focal length of the mirror is 441 mm at 180GHz.

## 2.4 ANGLES CORRECTION AT THE PLASMA EDGE

Due to the toroidal geometry the actual toroidal angles of the main beams of the Oblique ECE antenna at the plasma edge have a small but not negligible dependence on the geometrical location of the antenna itself, as shown in figure 3.

The input angle at the plasma edge is  $\alpha + \delta$  where  $\alpha$  is the angle at the antenna output and  $\delta$  is the angle to the centre of the tokamak of the impact point and is given by the expression:

$$\delta_b = \text{Arc tan} \left[ \frac{\text{Tan}(\alpha_b)(R_b - R_{\text{edge}}) - x_b}{R_{\text{edge}}} \right]$$

where the index  $b$  denotes the main beam ( $10^\circ$  or  $20^\circ$ ) and  $x_b$  is the offset of the launching point in toroidal direction. Assuming (in mm)  $R_{\text{edge}}=3882$ ,  $R_{10^\circ}=4336$ ,  $R_{20^\circ}=4315$ ,  $x_{10^\circ}=35.8$ ,  $x_{20^\circ}=49.1$  we find that  $\alpha_{10^\circ}=10.05^\circ$  and  $\alpha_{20^\circ}=22.27^\circ$ . The figures here used take into account the curvature of the last mirror and the actual path of the central rays of the two beams as calculated by the electromagnetic model. There are severe limitations in the possibility to decrease the actual  $20^\circ$  beam angle: decreasing the mirror 1 inclination would put the beam too close to the mirror 3 edge, causing edge diffraction. On the other hand increasing the mirror 3 inclination would cause mechanical interference with the external supporting structure of the whole antenna system.

In order to optimise the mirror dimensions to reduce diffraction effects, keeping into account the available space, the ellipsoidal mirror 3 has been designed with an asymmetrical rim shape, using the maximum available space towards the plasma edge as shown in figure 4.

## 3. ANTENNA PATTERN: PHYSICAL OPTICS CALCULATIONS.

The antenna model has been verified using the electromagnetic code GRASP8 [6]. The code is able to calculate the electromagnetic scattering from general structures, including successions of plane and curved reflectors. The analysis method used in the case of the Oblique ECE antenna is Physical Optics. The scattering analysis is a three step procedure where the first step is to calculate the surface currents induced on a reflector, the second step is to calculate the radiated field by these currents and the third step is to add the incident and the scattered field to calculate the total field. The first step is generally very time consuming for large reflectors. Physical Optics is a method to give an approximation to the surface currents valid for perfectly conducting scatterers that are large if compared with the wavelength, described by the equation (Collin and Zucker, [7]):

$$\mathbf{J}^e = 2\mathbf{N} \times \mathbf{H}^i$$

Where  $\mathbf{J}^e$  is the induced current,  $\mathbf{n}$  is the unit surface normal (outward from illuminated surface) and  $\mathbf{H}^i$  is the incident magnetic field. The radiated field can then be calculated from

$$\mathbf{E} = -j\omega(\mathbf{A}^e + \frac{1}{k^2} \nabla(\nabla \cdot \mathbf{A}^e)) - \frac{1}{\epsilon} \nabla \times \mathbf{A}^m$$

$$\mathbf{H} = \frac{1}{\mu} \nabla \times \mathbf{A}^e - j\omega(\mathbf{A}^m + \frac{1}{k^2} \nabla(\nabla \cdot \mathbf{A}^m))$$

Where  $\mathbf{A}$  is the vector potential,  $e$  and  $m$  denote electric and magnetic components,  $\pi^2 = k^2$ . In the

case of the Oblique ECE antenna the illuminating source is the beam propagating from a  $TE_{1,1}$  mode waveguide with aperture diameter of 32mm. The patterns generated by the two illuminating beams are calculated separately, despite the fact that the ellipsoidal mirror is shared. This procedure has been adopted to avoid undesired interference effects and is justified because the radiation received through the two lobes of the antenna is not coherent.

### 3.1 RESULTS AND CONCLUSIONS

Table 1 summarizes the results of the GRASP8 simulations. Beam radii (defined as the contours with  $-8.7\text{dB}$ ,  $\sim 1/e^2$ , attenuation with respect to the maximum) calculated at 1400mm from the ellipsoidal mirror of the antenna corresponding to the plasma edge position are reported in the upper side. The lower side shows an estimation of the angular spread in the toroidal direction, i.e. the maximum longitudinal extension of the  $-20\text{dB}$  contour around the actual angular direction of each of the main beams of the antenna.

In the figure 5 the antenna pattern calculated at 300mm (first row) and at 1400mm (second row) from the ellipsoidal mirror are shown. Apart from small deformations of the main lobes at level of  $-18\text{dB}$ , the secondary lobes are at least 24dB below the maximum. Performances of the ECE Oblique antenna as evaluated with the simulations above are compliant with the physics requirements of the diagnostics. This work has been partially supported with the EFDA contract JW4-NEP-ENE-37

### REFERENCES

- [1]. G. Taylor et al., Proc. 9th Joint Workshop on ECE and ECRH, Borrego Spring (1995) p.485
- [2]. E. de la Luna et al., Impact of bulk non-Maxwellian electrons on electron temperature measurements, Rev. Sci. Instrum. **74** (2003) p. 1414
- [3]. O. Tudisco et al., Electron Cyclotron Heating experiments during the current rampup in FTU, 26th EPS Conf. on Contr. Fusion and Plasma Physics, Maastricht (1999), ECA Vol.23J (1999) pp. 101-104
- [4]. E. de la Luna, O. Tudisco, et al. Diagnosing the electron distribution function with oblique electron cyclotron emission on FTU. Proceedings of the 12th Joint Workshop on Electron Cyclotron Emission and Electron Cyclotron Heating (ed. by G. Giruzzi, World Scientific, Singapore, 2003), p. 024.
- [5]. V. Krivenski, Electron cyclotron emission by non-Maxwellian bulk distribution functions, Fusion Engineering and Design **53** (2001) p. 23
- [6]. K.Pontoppidan (Editor), GRASP8 Technical Description, DTK, 2002, Copenhagen pp. 155-164, [www.ticra.com](http://www.ticra.com)
- [7]. R.E. Collin and F.J. Zucker, Antenna Theory, Part 1, Chapter 1, McGraw-Hill, 1969, New York



Table 1: Summary of the antenna performances (see text).

(a) Equivalent gaussian beam radius (mm)				
Beam	100 GHz	130 GHz	200 GHz	400 GHz
20° - x	86.7	66.4	44.7	24.0
20°	95.6	76.3	53.0	28.9
10° - x	97.0	74.7	49.8	34.7
10° - y	87.5	72.3	49.8	27.3
(b) Angular spread (°)				
Beam	100 GHz	130 GHz	200 GHz	400 GHz
20° - x	9.1	6.8	4.6	2.5
10° - x	9.5	7.8	4.4	3.1

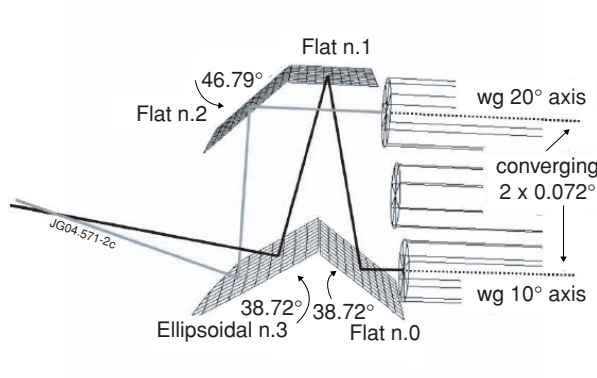


Figure 1. Physical optics model of the ECE oblique antenna. Angles are referred to the central waveguide axis.

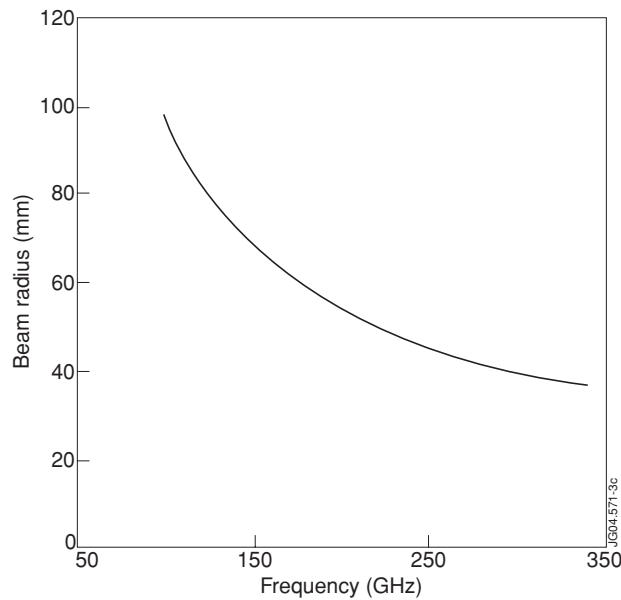


Figure 2. Beam radius ( $1/e$  2 of the radial power distribution) for an ellipsoidal mirror of 500mm focal length calculated at 1500mm from the waveguide aperture. The mirror is assumed at 140mm from the waveguide aperture.

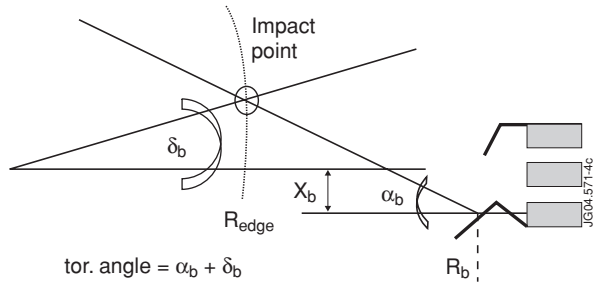


Figure 3. Toroidal angular correction for the antenna main beams.

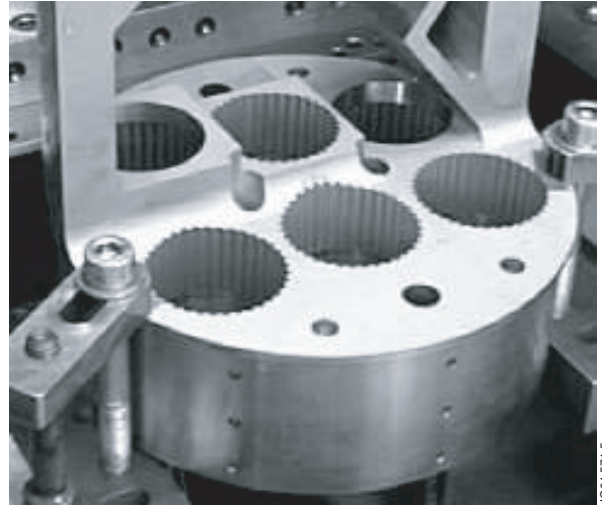


Figure 4. ECE oblique antenna, built from a single aluminum piece together with the terminal part of the waveguides. Courtesy Thomas Keating Ltd.

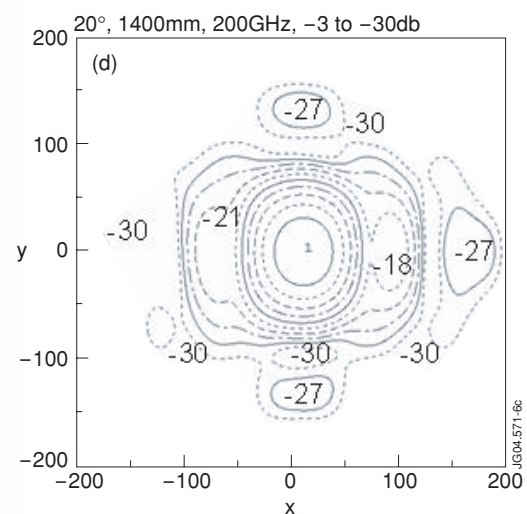
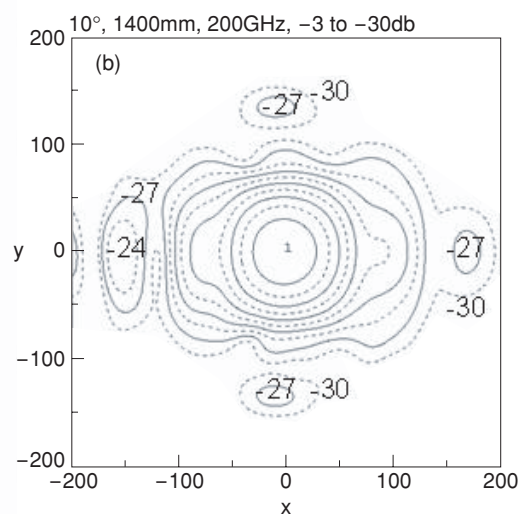
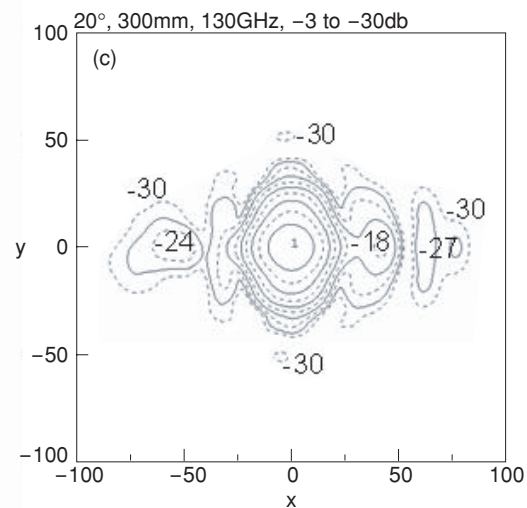
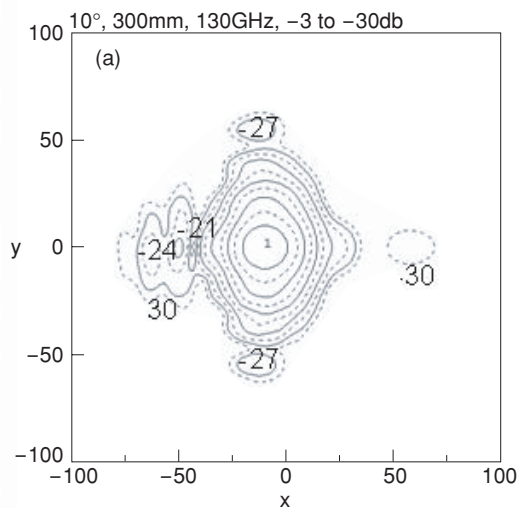


Figure 5. Contour plots of the calculated antenna patterns. In the first row the full scale of the plot is 200x200 mm, in the second row is 400x400mm. Each contour line marks a 3dB decrease in the intensity relative to the maximum.